Cluster studies of the interaction of oxygen with the lithium (100) surface

K. Hermann* and P. S. Bagus
IBM Research Laboratory, San Jose, California 95193
(Received 29 August 1977)

The interaction of an oxygen atom with the lithium (100) surface is studied using cluster models. On the basis of *ab initio* Hartree-Fock–linear-combination-of-atomic-orbitals theory the electronic structure of Li_n and Li_nO clusters ($n \leq 9$) is calculated for the three high-symmetry surface positions of the oxygen: on top, central, and bridge positions. The geometry of the Li centers in the clusters is chosen to represent a section of the bcc crystal at the (100) surface. The oxygen distance perpendicular to the surface in Li_nO is optimized with respect to the cluster total energy. The changes of various properties of the adsorption of O on the Li_n clusters, in particular binding energy and equilibrium distance from the surface, are considered as a function of the number of atoms, n, in the substrate cluster. The differences among these properties for the different adsorption sites are rather large and much larger than the changes obtained for the same site with different size Li_n clusters. The Li-O bond is always highly ionic. In the on-top position the oxygen becomes stable as O^- with a binding energy $D \approx 1.5$ eV. In the central position the oxygen stabilizes in the surface plane as O^{2-} with $D \approx 3$ eV. In the bridge position the oxygen penetrates as O^{2-} into the substrate with $D \approx 5$–6 eV. The results indicate that upon adsorption in the bridge position the oxygen penetrates into the lithium (100) surface and stabilizes as O^{2-} with a high binding energy. This gives a reasonable first step of the metal oxidation which in the real situation happens spontaneously. The energy of the oxygen vibrations normal to the surface is similar for the on-top and central positions (≈ 53 meV), whereas the value for the bridge position is much smaller (≈ 29 meV). This difference can be understood on the basis of simple geometric arguments.

I. INTRODUCTION

A quantitative description of the interaction between atoms (or molecules) and a solid surface is essential to the understanding of adsorption processes and chemical reactions on the surfaces. These are of both scientific and technological interest. Important examples are catalysis and corrosion.

An exact quantum-mechanical treatment of the real adsorbate–solid-substrate system is not possible. Therefore, a number of approximations and simplifications have to be introduced to make the system tractable. The methods that are used to determine the adsorbate-substrate interaction can be divided into three groups differing essentially by the approximations used to treat the many-electron system.

The first group comprises those methods where the electron-electron interaction in the infinite substrate is described by local potentials. This applies for adsorption calculations with the density-functional formalism[1-3] as well as for methods where the (two-dimensionally periodic) substrate is described by band-structure-type formalisms.[4-8] The second group contains semiempirical chemisorption theories where the electron-electron interaction is described by simple model Hamiltonians, e.g., the Anderson[9] or the Hubbard[10] model. These models have been first applied to chemisorption problems by Grimley.[11] Further, Schrieffer[12] proposed the induced-covalent-bond (ICB) theory which is a natural generalization of the Heitler-London theory for diatomic molecules. In most cases the matrix elements of the electronic interaction in these theories are treated as fitting parameters to match with experimental data. A review on the different models and their results has been given in a number of papers.[11,13]

If we suppose that the adsorbate-substrate interaction is localized to a few substrate atoms near the surface, we can approximate it by the interaction in a fictive molecule (cluster) which contains only the adsorbate and a few substrate atoms. The coupling of this "surface molecule"[14] to the rest of the substrate has to be included in a second step, the embedding problem.[15] Alternatively, one could increase the surface cluster by adding substrate atoms until the chemisorption properties become independent of cluster size.

This concept of the surface molecule forms the basis of the third group of chemisorption models. In a number of publications surface clusters have been studied with standard quantum-chemical methods neglecting the coupling of the cluster to the rest of the substrate. We mention here surface cluster studies using extended Hückel,[16-20] complete neglect of differential overlap (CNDO),[16,21,22] multiple-scattering–$X\alpha$ (MS$X\alpha$),[23,24] discrete variational,[25,26] and *ab initio* Hartree-Fock–linear combination of atomic orbitals (LCAO) methods.[27-34]

The difficulty of cluster calculations increases substantially as the size of the cluster is increased. Thus, very few systematic studies of the convergence of cluster properties with respect to size have been performed. Messmer *et al.*,[35] using the MS$X\alpha$ method, report that for transition metals 10 to 15 atom clusters are sufficiently large to describe the bulk electronic density of states reasonably well. In contrast, Hartree-Fock studies[29] show that the properties of a Be_{22} cluster are considerably different from those of the bulk. For clusters which are designed to model chemisorption, it is necessary to know how many substrate atoms are required for the calculated chemisorption properties to converge. Grimley *et al.*[22] report, based on a CNDO study on Li_nH ($n \leq 22$), that the chemisorption energy of hydrogen varies only by 10% if the cluster size is increased from 10 to 20 substrate atoms. A similar result has been found by Bauschlicher *et al.*[29] from a Hartree-Fock–LCAO study on Be_nH ($n \leq 22$). They conclude that once all the substrate atoms nearest to the adatom (the atoms involved in the local substrate-adsorbate bonding) are interior atoms of the cluster, then the chemisorption properties will change only slightly with further increase in cluster size.

In the present paper, we study the interaction of an oxygen atom with the lithium (100) surface with cluster models. The *ab initio* Hartree-Fock–LCAO method is used to calculate the electronic structure of different Li_n and Li_nO clusters ($n \leq 9$). From these calculations, the equilibrium distance and binding energy of the oxygen is determined for the three-high-symmetry surface sites: on-top, central, and bridge positions. Further, the ionicity of the adsorbed oxygen as well as its energy for vibrations perpendicular to the surface is calculated. A comparison of the Li_nO results shows characteristic differences of the chemisorption parameters for the three sites. These differences are larger than the variation of the results between different clusters for the same adsorption site. This seems to justify a generalization of the cluster results to the situation on the surface although the clusters that have been studied are still too small to give a reliable description of the substrate surface.

It is well known from elementary chemistry that if metallic lithium is exposed to oxygen, lithium oxide (Li_2O) is formed spontaneously. This makes it experimentally difficult to obtain clean and well-defined lithium crystals or films, as well as to carry out experimental studies with oxygen. For this reason there are no experimental data available to compare with our calculations. However, the oxygen-lithium system might become technologically interesting for the construction of fusion reactors.[36,37] The present paper is the first systematic model study of the reactive adsorption of oxygen on lithium. Results for lithium clusters as large as Li_{13} have been published previously.[38] Further, Quinn *et al.*[39] have calculated the shifts of the oxygen core ionization potentials due to the interaction with lithium in Li_nO clusters ($n \leq 5$) using the MS$X\alpha$ method. However, they seem to have chosen quite unreasonable values for the oxygen position in the clusters and did not carry out any geometry optimization. A preliminary report on the present results has been given recently.[34]

In Sec. II, we discuss the computational details of our calculations. The geometry of the clusters is given in Sec. II A. Sections II B–II E present the details of the electronic structure calculations, choice of basis sets, symmetry considerations, and the problem of identifying the cluster ground state. In Sec. III we present our results. Section III A discusses the results of the pure Li_n substrate clusters; in Secs. III B–III D the Li_nO data are presented for the three different oxygen symmetry positions. Finally, in Sec. IV, we compare the Li_nO results for the different oxygen symmetry positions and give our conclusions for adsorption on the lithium (100) surface.

II. COMPUTATIONAL DETAILS

A. Geometry of the Li_n and Li_nO clusters

The positions of the Li centers in the clusters are chosen to reproduce the unreconstructed bcc structure of lithium at the (100) surface (cf. Fig. 1) where the Li bulk value for the lattice constant, 6.614 bohrs,[40] is used. This assumes that the lattice is not significantly distorted at the surface, a situation which has been found from low-energy electron-diffraction (LEED) studies to be the case for

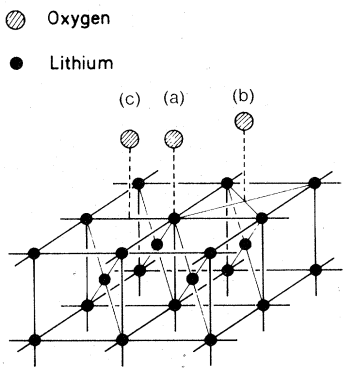

FIG. 1. Schematic representation of the (100) surface of bcc lithium indicating the three high-symmetry surface positions: (a) on top position; (b) central position; and (c) bridge position.

a number of metal surfaces.[41] For lithium itself, there are no experimental data available.

As possible surface sites for the adsorbed oxygen atom, we consider the three high-symmetry points of the (100) surface as shown in Fig. 1. (a) We consider a position directly above a Li center on the first substrate layer (on-top position). The surface normal at this position forms a fourfold symmetry axis of the substrate. (b) We consider a position directly above a Li center of the second substrate layer (central position). The surface normal at this position also forms a fourfold symmetry axis of the substrate. (c) We consider a position along the surface normal bisecting the line between two nearest neighbors of the first substrate layer (bridge position). The surface normal forms a twofold symmetry axis of the substrate.

For these oxygen positions Li_nO clusters are chosen such that the lithium part represents a section of the crystal at the (100) surface and has the full surface symmetry (characterized by C_{4v} and C_{2v}, respectively) with respect to the adsorbate position. For the following, we shall denote the clusters by

$$Li_nO(k_1, k_2, \ldots) \text{ and } Li_n(k_1, k_2, \ldots),$$

where k_i gives the number of Li atoms of the ith substrate layer that are present in the cluster. Obviously, the reaction

$$\sum_i k_i = n$$

holds for all clusters. The expression "Li atom of the ith layer in the cluster" will be used frequently in the following. Figures 2(a)–2(c) show the geometric structure of all Li_nO clusters that

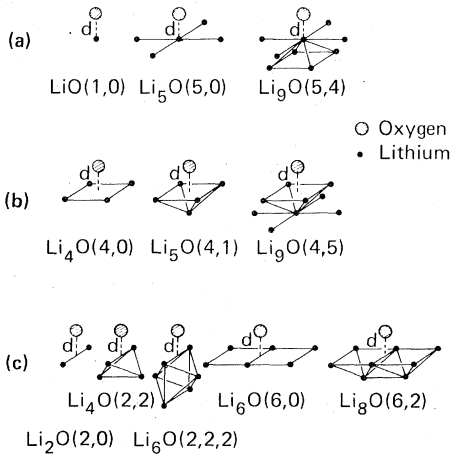

FIG. 2. Size and structure of the Li_nO clusters used: (a) oxygen in the on top position; (b) central position; and (c) bridge position. The adsorbate distance d is shown for each cluster.

are used in the present study: three different clusters for the on-top and central position, and five different clusters for the bridge position. The distance d of the oxygen center with respect to the substrate surface is defined as the distance along the surface normal for a given site from the first layer of substrate atoms. The equilibrium value of d, d_{min} is determined for each cluster by minimizing the total energy of the cluster with respect to variations in d. The structures of the respective Li_n substrate clusters follow from those of the Li_nO clusters in the limit $d \to \infty$.

B. Calculations of the electronic structure of a cluster

For the calculation of the electronic states in the clusters we use the self-consistent-field (SCF) Hartree-Fock-(HF)[1] LCAO method described by Roothaan for both closed-[42] and open-shell[43] systems. It has proven to give reasonably accurate results for both geometric and energetic quantities in a large number of free molecules.[44] Thus, it is reasonable to apply this method to surface cluster problems. The SCF-HF-LCAO method is implemented in the program system MOLALCH[45] which is used for all cluster calculations of the present study.

All calculations have been performed for spin restricted[42,43] HF wave functions. That is, the spatial parts of the α and β spin orbitals of doubly occupied (closed) shells were required to be the same. In some cases, the spatial parts of orbitals belonging to degenerate representations (π, e, etc.) were also required to be equivalent.[43,44] The choice of symmetry and equivalence restrictions is discussed further in Sec. II D.

C. Basis-set considerations

In cluster calculations using LCAO methods the choice of an appropriate basis set for the representation of the molecular orbitals (MO's) is of vital importance for the accuracy of the results. This applies in particular to larger clusters where, for computational reasons, the basis set cannot be extended arbitrarily. In the present calculations, we used contracted Gaussian basis sets described below.

The exponents and contraction coefficients for the s orbitals of lithium are taken from Van Duijneveldt's[46] calculations on the free atom. An optimized 9s basis was contracted to 4s (6,1,1,1) in the usual way.[47] Using this basis set, we get for the ^2S ground state of the atom a total energy of −7.432144 hartree (Van Duijneveldt's original value is −7.432413 hartree). For comparison the spin restricted Hartree-Fock limit is −7.432728 hartree.[48] In order to obtain reasonable descrip-

tions of the Li-Li and the Li-O bonds in the clusters, the Li basis is expanded by including p-type functions. The exponents and contraction coefficients are taken from calculations on the excited $^2P(1s^2 2p^1)$ state of the atom where an uncontracted $9s4p$ basis has been optimized.[49] The four p basis functions are contracted to $2p$ (3, 1) for a basis A and to $3p$ (2, 1, 1) for a basis B. The exponents and contraction coefficients for both basis sets are given in Table I. The differences in the results for the two basis sets will be discussed below for the LiO molecule.

We expect that oxygen will be ionic in the Li_nO clusters due to its large electronegativity with respect to lithium. Therefore, we have taken the oxygen basis set from a basis optimization of the free O^- ion.[50] Here an uncontracted $9s$ $5p$ basis is contracted to $4s$ (5, 2, 1, 1) and $3p$ (3, 1, 1). The exponents of this basis are slightly smaller compared to those optimized for the neutral atom.[46] As a consequence, the difference in the total energy of the oxygen ^3P ground state (−74.796 053 hartree) with respect to the Hartree-Fock limit (−74.809 41 hartree)[48] is larger than for lithium.

We do not include d-type orbitals in our basis sets as the effect on the Li-O or Li-Li bond due to admixing of d contributions is likely to be small in the clusters. This assumption has been confirmed by HF and configuration interaction (CI) studies on Li_2,[51] and LiO,[52] respectively. The inclusion of d orbitals in the basis set would have led to a considerable increase in complexity of the calculations, particularly for the larger clusters.

To test the accuracy of the basis sets, we have studied the Li-O interaction in diatomic LiO. Figure 3 gives the potential energy of the $^2\Pi$ ground state of the molecule as a function of the interatomic separation near the equilibrium distance. The HF $^2\Pi$ state does not converge to the dissociation limit [Li(^2S), O(^3P)]. Therefore, we use the sum of the two atomic total energies as a reference for infinite separation. A comparison of the two curves for the Li basis sets $A(4s2p)$ and

TABLE I. Exponents and contraction coefficients of the basis sets for Li and O. The functions are denoted as $C_1(\alpha_1) + C_2(\alpha_2) + \cdots$ where C_i are the contraction coefficients and α_i the exponents. See Ref. 44 for a more complete definition of contracted Gaussian basis sets. The p functions for Li basis sets A and B are listed separately.

Atom	Type	Function
Li	S	0.000 844(1359.446 6) + 0.006 485(204.026 47) + 0.032 466(46.549 541) + 0.117 376(13.232 594) + 0.294 333(4.286 148) + 0.450 345(1.495 542)
	S	1.0(0.542 238)
	S	1.0(0.073 968)
	S	1.0(0.028 095)
	Set A P	0.037 973(1.534 300) + 0.231 890(0.274 990) + 0.834 779(0.073 618)
	Set A P	1.0(0.024 026)
	Set B P	0.037 973(1.534 300) + 0.231 890(0.274 990)
	Set B P	1.0(0.073 618)
	Set B P	1.0(0.024 026)
O	S	0.000 800(10 662.3) + 0.006 152(1599.71) + 0.031 161(364.725) + 0.115 581(103.652) + 0.301 659(33.9058)
	S	0.444 516(12.2875) + 0.243 771(4.756 80)
	S	1.0(0.956 700)
	S	1.0(0.261 150)
	P	0.015 726(32.512 70) + 0.100 721(7.156 66) + 0.313 428(2.022 02)
	P	1.0(0.582 465)
	P	1.0(0.140 924)

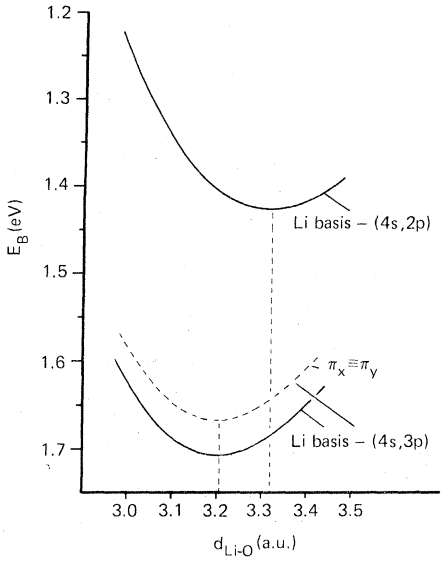

FIG. 3. Potential curves of the LiO ($^2\Pi$) state computed with the two lithium basis sets. In addition the curve of the $(4s, 3p)$ basis is given where equivalence restrictions are imposed on the 1π orbitals ($\pi_x \equiv \pi_y$, dashed curve).

$B(4s3p)$ shows their different flexibility. The binding energy D for basis set B, 1.708 eV, is 20% larger than that for basis set A, 1.428 eV; the equilibrium positions $d_{\min}$ also differ significantly: set A gives $3.320a_0$ and set B gives $3.206a_0$. This indicates a considerable improvement in the description of the Li-O interaction if basis set B is used instead of A.

Our HF results with basis set B are in very good agreement with those obtained by Yoshimine[52] who used an extremely flexible basis set of Slater-type[44] orbitals including functions up to $l = 3$. Yoshimine finds $d_{\min} = 3.162a_0$ and $D = 1.87$ eV; these Hartree-Fock limit values are within 1% of our $d_{\min}$ and 0.16 eV or 9% larger than our D. Thus we expect that our basis set B will give results quite close to the Hartree-Fock limit values for the larger Li_nO clusters and all further calculations were performed with this basis set. This permitted us to study clusters with up to 9 Li atoms using reasonable amounts of computer time.

It is also interesting to compare the HF results with accurate CI results[52] for LiO. The CI $d_{\min} = 3.203a_0$ is quite close to both our and Yoshimine's HF value. The CI $D = 3.41$ eV is ~1.5 eV larger than the HF value. This is consistent with the accuracy usually expected of HF wave functions.[44] Thus it is reasonable to expect that our computed $d_{\min}$'s for the Li_nO clusters will be rather reliable and that the computed D's will be too small by ~1–2 eV.

A more detailed study of the electronic structure of LiO shows an almost ionic Li-O bond with a charge transfer of roughly one electron. The Mulliken analysis gives $Li^{+0.81}O^{-0.81}$. This result justifies the choice of the oxygen basis set.

D. Symmetry considerations

As has been mentioned in Sec. IIA, the symmetry behavior of the Li_nO clusters is described by the point group C_{2v} (oxygen bridge position) or C_{4v} (oxygen on-top and central position) except for LiO ($D_{\infty h}$). Thus, in all calculations symmetry adapted basis functions are used which transform according to the irreducible representations of the cluster point group.

For the electronic structure of the pure Li_n substrate clusters, we always use the point group of the respective Li_nO which in some cases does not give the full Li_n symmetry. As an example, we mention $Li_4(2, 2)$ which is calculated in C_{2v} symmetry, although it has S_4 symmetry. However, the many-electron wave functions always had the full Li_n cluster symmetry.

For clusters with open-shell ground states, the electronic total charge density may transform according to a symmetry representation other than 1 (= unit representation) unless certain symmetry equivalence restrictions are imposed on the one-electron functions. An example is the $^2\Pi(4\sigma^2 1\pi^3)$ ground state of LiO. Here the charge density of a configuration $^2\Pi(4\sigma^2 1\pi_x^2 1\pi_y^1)$ does not have the full rotational symmetry of the molecule and the one-electron functions $1\pi_x$ and $1\pi_y$ are slightly different in their radial $[F(\rho, \theta)$ in cylindrical coordinates] behavior. Imposing an equivalence restriction requiring that the radial parts, $F(\rho, \theta)$, of $1\pi_x$ and $1\pi_y$ be identical (effective one-electron occupations of $1\pi_x^{1.5} 1\pi_y^{1.5}$) gives a total energy which is higher by only 0.05 eV compared to $^2\Pi(4\sigma^2 1\pi_x^2 1\pi_y^1)$. This can be seen from Fig. 3, where the LiO binding curves are shown for both configurations.

In test calculations performed to determine the ground state of a cluster, we usually did not impose the symmetry equivalence restriction for open-shell configurations. However, once an open-shell ground state had been determined, we also performed the Hartree-Fock calculations with the equivalence restriction. For all the clusters considered, the increase in the total energy due to imposing the restriction was always less than 0.05 eV. This is too small to merit further consideration.

E. Determination of the cluster ground state

The determination of the electronic ground-state configuration is one of the main problems in clus-

ter calculations. Quantum-chemical intuition which is successful in predicting the ground state of small molecules with closed-shell structure can fail for larger clusters. In the present study we apply a careful procedure to identify the cluster ground state.

For a given cluster A we started with a highly ionic state Φ^p, the ground state of the "core cluster" A^{p+} where only the cluster core orbitals [Li(1s) and O(1s) and O(2s)] are occupied. This state with only closed shells is very easy to obtain when the core orbitals of the respective free atoms are used as trial MO's.

In a next step, we calculated a wave function Φ^{p-k} of $A^{(p-k)+}$ ($k=1$, 2, or 3) where as trial MO's we used the one-electron orbitals of Φ^p plus the energetically lowest virtual orbital(s) of A^{p+}. The orbitals of Φ^{p-k} plus one or two additional virtual orbitals of $A^{(p-k)+}$ then served as input to determine a wave function of the less ionized cluster $A^{(p-k-l)+}$. This procedure was repeated until a wave function $\Phi^0(\equiv\Phi_0)$ for the neutral cluster A was obtained. This usually took three to six steps.

In order to test whether Φ_0 is actually the ground state of the cluster we examined a large number of alternative configurations. As an MO basis we used the occupied orbitals of Φ_0 plus, depending on the cluster, four to eight of the energetically lowest virtual orbitals. We constructed the additional configurations Φ_n by removing electrons from the occupied MO's of Φ_0 and placing them into the virtual MO's subject to the constraint that the Li(1s) and O(1s) core orbitals were always doubly occupied. We considered all possible configurations which could be formed by placing one or two electrons into the virtual MO's. Configurations Φ_n for all representations of the cluster point group, but only for the two lowest spin multiplicities, were allowed. That is, we considered singlet and triplet states for even electron systems, and doublet and quartet states for odd electron systems. Wave functions with higher multiplicity are not likely to be ground states since lithium metal does not have a net spin moment in the ground state. For the larger Li_n and Li_nO clusters, we have examined between 1500–3000 different wave functions Φ_n per cluster.

For each Φ_n, we calculated the expectation value of the total Hamiltonian

$$H_{nn}=\langle\Phi_n|H|\Phi_n\rangle;\quad n=1,2,\ldots.$$

The order of the energy expectation values H_{nn} ($n=0,1,2,\ldots$, where $H_{00}=\langle\Phi_0|H|\Phi_0\rangle$) gives a first indication about the ground state of the cluster A. However, the wave functions $\Phi_n(n>0)$ are not self-consistent solutions of the Hartree-Fock equations. Thus, the expectation value H_{nn} will be higher (less negative) than that obtained as a self-consistent solution of the Hartree-Fock equations for the configuration Φ_n. We denote the HF energies and wave functions for this configuration as $\tilde{H}_{nn}$ and $\tilde{\Phi}_n$. For the three to five configurations with the lowest values of H_{nn}, we now obtained the self-consistent results $\tilde{H}_{nn}$. If the lowest total energy of these $\tilde{H}_{nn}$ was greater than H_{00}, then Φ_0 and H_{00} were clearly identified as the ground-state energy and wave function of A. If the lowest energy, say $\tilde{H}_{mm}$, was lower than H_{00}, it was necessary to continue the search for the ground state. We treated $\tilde{\Phi}_m$ as a new test ground state Φ_0 and repeated the search procedure over configurations Φ_n as described above. In all cases, one to three steps were needed to find the cluster ground state.

For the Li_nO clusters, the ground-state configuration was determined for only one reasonably chosen distance d of O from the Li_n cluster. This ground-state configuration was used for all other values of d. The trial MO's for starting the Hartree-Fock calculation at a new distance were those obtained as the solutions at a nearby value. Calculations were performed for various distances to obtain an interaction potential curve about the equilibrium distance $d_{\min}$.

III. RESULTS AND DISCUSSION

A. Li_n clusters

The total energy $E_{\text{tot}}(Li_n)$ and the electronic configuration, specified by showing the highest occupied orbital of each irreducible representation, of the ground states of the Li_n clusters are given in Table II. In addition, we give the sum of the atomic Hartree-Fock energy of n Li atoms, $nE_{\text{tot}}(\text{Li})$. In Table III, we give the total cluster binding energy

$$B=-[E_{\text{tot}}(Li_n)-nE_{\text{tot}}(\text{Li})]$$

and the binding energy per atom $b=B/n$.

For Li_2 at $d=6.614a_0$ (the lithium-metal lattice constant), the cluster in the Hartree-Fock approximation is energetically unstable; $b=-0.07$ eV. This is a consequence of two related facts. First, the Hartree-Fock $^1\Sigma_g^+$, $1\sigma_g^2 1\sigma_u^2 2\sigma_g^2$ ground state of Li_2 does not dissociate to two Li(^2S) atoms. The wave function, at large separation, is 50% Li(^2S) + Li(^2S) and 50% $Li^+(^1S)$ and $Li^-(^1S)$. As a consequence, the Hartree-Fock energy at large separation is higher than that of two Li(^2S) atoms by $\frac{1}{2}J(2s,2s)$ which is the Coulomb repulsion introduced by the $Li^-(^1S)$ term in the wave function. [The value of $J(2s,2s)$ for the 2s orbital of Li(^2S) is 0.23 hartree = 6.4 eV.] Second, correlation effects contribute[53] approximately 70% of the dis-

TABLE II. Ground-state symmetry, configuration, and total energy $E_{\text{tot}}(\text{Li}_n)$ of the lithium clusters without oxygen. The energy of n Li(^2S) atoms $nE_{\text{tot}}(\text{Li})$ is given for comparison. The configuration is described by giving only the last molecular orbital in each irreducible representation. Energies are in atomic units; 1 hartree = 27.2116 eV.

Cluster	Point-group symmetry	Ground state	Configuration	$E_{\text{tot}}(\text{Li}_n)$	$nE_{\text{tot}}(\text{Li})$
Li	$O(3)$	^2S	$2s^1$	−7.432 143 6	−7.432 143 6
Li_2	$D_{\infty h}$	$^1\Sigma_g^+$	$1\sigma_u^2 2\sigma_g^2$	−14.861 667 1	−14.864 287 2
$\text{Li}_4(4,0)$	C_{4v}	$^3A_2$	$2a_1^2 2e^2 1b_2^2$	−29.738 001 8	−29.728 574 4
$\text{Li}_4(2,2)$	C_{2v}	$^3A_2$	$3a_1^2 2b_1^1 2b_2^1$	−29.752 703 8	−29.728 574 4
$\text{Li}_5(5,0)$	C_{4v}	$^4B_2$	$3a_1^2 2b_1^1 2e^2$	−37.162 643 7	−37.160 718 0
$\text{Li}_5(4,1)$	C_{4v}	^2E	$3a_1^2 2e^3 1b_2^2$	−37.189 312 2	−37.160 718 0
$\text{Li}_6(6,0)$	C_{2v}	$^3B_2$	$3a_1^2 3b_1^1 2b_2^2 2a_2^1$	−44.609 382	−44.592 861 6
$\text{Li}_6(2,2,2)$	C_{2v}	$^3B_2$	$5a_1^1 3b_1^2 2b_2^1$	−44.646 220 5	−44.592 861 6
$\text{Li}_8(6,2)$	C_{2v}	$^3B_2$	$5a_1^2 3b_1^1 3b_2^2 2a_2^1$	−59.520 262 8	−59.457 148 8
$\text{Li}_9(5,4)$	C_{4v}	$^2A_1$	$5a_1^1 3e^4 2b_1^2 1b_2^2$	−66.988 690 7	−66.889 292 4

sociation energy of Li_2. Thus the Hartree-Fock total energy of Li_2 at equilibrium separation ($d = 5.26a_0$) is lower by only 0.2 eV compared to the dissociation limit (the experimental dissociation energy is ≈1 eV), and for separations $d > 6a_0$ the total energy of Li_2 ($^1\Sigma_g^+$) lies above the dissociation limit. At all reasonable internuclear separations, the configuration $1\sigma_g^2 1\sigma_u^2 2\sigma_u^2$ makes a large contribution to the correlation energy. At large separations, it makes the dominant contribution since this is the configuration required for proper dissociation to ground state separated Li(^2S) atoms.[53] (In contrast to the poor Hartree-Fock result for the dissociation energy the electron charge density of Li_2 should be reasonable near the equilibrium position. This is supported by the fact that the vibrational frequencies and the equilibrium distance agree fairly well with experiment.[53])

Both the incorrect dissociation and the lack of correlation in Hartree-Fock theory will lead in all Li_n clusters to a cluster binding energy B which is too small. However, as may be seen from Table III, all Li_n clusters except Li_2 are stable with respect to the dissociated atoms. Thus, it is possible that the Hartree-Fock binding-energy errors may be smaller in these clusters. In order to obtain an estimate of the correlation correction in the largest cluster, we have carried out small valence electron CI calculations on Li_9. As a basis we used the occupied orbitals of the $^2A_1$ ground state of Li_9 and the three energetically lowest virtual orbitals of the (self-consistent) $^1A_1$ ground state of Li_9^+. In the CI calculations, we included all configurations (of the appropriate symmetry) which could be formed by making single and double excitations from the occupied valence orbitals of Li_9 into the virtual orbitals. The CI energy of the $^2A_1$ ground state is only 0.16 eV lower than the Hartree-Fock value. This suggests that the correlation corrections to B may be small for the larger Li_n clusters. However, for a quantitative study of the importance of correlation in Li_n more extensive CI calculations are necessary than have been carried out.

It is clear from Table III that the binding energy per atom b is, for all clusters, much smaller than the experimental cohesive energy of lithium metal 1.6 eV.[54] However, the values of b cannot be compared with the bulk cohesive energy because most of the atoms in the Li_n clusters are geometrically

TABLE III. Binding energies of the Li_n clusters. The total energy lowering B is taken with respect to n separate atoms. The binding energy per atom is $b = B/n$. The negative value for Li_2 indicates that it is unstable within the Hartree-Fock approximation.

Cluster	B (eV)	b (eV)
Li_2	−0.071	−0.036
$\text{Li}_4(4,0)$	0.257	0.064
$\text{Li}_4(2,2)$	0.657	0.164
$\text{Li}_5(5,0)$	0.052	0.010
$\text{Li}_5(4,1)$	0.778	0.156
$\text{Li}_6(6,0)$	0.450	0.075
$\text{Li}_6(2,2,2)$	1.452	0.242
$\text{Li}_8(6,2)$	1.717	0.215
$\text{Li}_9(5,4)$	2.705	0.301

inequivalent. In particular, even in the largest clusters none of the atoms possesses the complete nearest- and next-nearest-neighbor environment of the metal. We can, however, fit our calculated results using a very simple model which takes into account only nearest and next-nearest-neighbor pair interactions. We assume that the contribution of atom i to the total cluster binding energy W_i is given by

$$W_i = n_{i1}A_1 + n_{i2}A_2 ,$$

where n_{i1} (n_{i2}) is the number of nearest-(next-nearest-) neighbor atoms in the cluster. The energies A_1 and A_2 characterize the interaction between two atoms at the respective distances. In this model the total energy lowering is given by

$$B_{\text{approx}} = \sum_i W_i = \left(\sum_i n_{i1}\right)A_1 + \left(\sum_i n_{i2}\right)A_2 = N_1 A_1 + N_2 A_2 .$$

From a least-squares fit of B_{approx} with the computed B of Table III for all clusters except Li_2, we get

$$A_1 = 0.085 \text{ eV}; \quad A_2 = 0.026 \text{ eV}.$$

Table IV gives N_1, N_2 for all clusters and compares B_{approx} with B. For most of the clusters, B and B_{approx} agree reasonably well. Thus the pair interaction model would appear to form the basis of a reasonable interpolation scheme. [The agreement between B and B_{approx} is worst and rather poor for Li_2 and $Li_5(5,0)$. These are open clusters and we discuss below why we expect the pair interaction model to be particularly poor for them.] If we use the above model for an atom in lithium metal the cohesive energy E_c is given by

$$E_c = 8A_1 + 6A_2 ,$$

which gives a numerical value of 0.84 eV or 50% of the experimental cohesive energy. The discrepancy between extrapolation and experiment is due to the difference in the boundary conditions for the cluster and the solid, the neglect of correlation, and the limitations of the pair interaction model.

A brief comment on the pair interaction model is in order. We would certainly expect that three-particle, four-particle, and higher-order interactions would contribute importantly to the cohesive energy of a metal. For Be clusters, Kolos *et al.*[55] have shown, for interatomic distances appropriate to Be metal, that the magnitude of the three-particle interaction is actually larger than the pair interaction energy. Thus, A_1 and A_2 must be regarded as empirical fitting parameters which include the effect of higher-order interactions. This is obvious if we compare the values of $2A_1$ and $2A_2$ with the Li_2 binding energies at the appropriate distances (see this work, above, and Ref. 53). Thus the fitted value A_2 will be meaningless for Li_2. The $Li_5(5,0)$ cluster is the only $n > 2$ cluster which does not contain a square Li_4 four-body contribution. Hence, we would expect the fit to be poor for $Li_5(5,0)$ if the four-body term is important. It appears likely that this may be the case.

Edge effects (that is, the fact that the peripheral atoms of a cluster have an atomic environment different from more-central atoms) influence the cluster electronic properties in many other ways. Their importance can also be seen from the cluster first ionization potentials I_{min}. The results given in Table V are multiplet average values where the orbital relaxation in the final state is neglected. For all clusters except for the atom, I_{min} gives 4.1 ± 0.4 eV with a trend towards smaller values if the cluster size is increased. However, the variation of I_{min} is still large for the larger clusters [$Li_6(2,2,2)$:4.17 eV, $Li_8(6,2)$:3.78 eV, $Li_9(5,4)$:3.91 eV]. This result becomes obvious if we study the spatial charge distribution of the respective cluster orbitals that are ionized. Population analyses and charge-density plots show that

TABLE IV. Numerical results for the interpolation of the total energy lowering in Li_n. The definitions of the quantities are given in the text.

Cluster	N_1	N_2	B_{approx} (eV)	B (eV)
Li_2	0	2	0.052	−0.071
$Li_4(4,0)$	0	8	0.208	0.257
$Li_4(2,2)$	8	4	0.784	0.657
$Li_5(5,0)$	0	8	0.208	0.052
$Li_5(4,1)$	8	8	0.888	0.778
$Li_6(6,0)$	0	14	0.364	0.450
$Li_6(2,2,2)$	16	10	1.620	1.452
$Li_8(6,2)$	16	16	1.776	1.717
$Li_9(5,4)$	24	16	2.456	2.705

TABLE V. First ionization potential I_{min} for Li_n computed in the frozen-orbital approximation.

Cluster	Ionized orbital	I_{min} (eV)
Li	$2s$	5.335
Li_2	$2\sigma_g$	4.524
$Li_4(4,0)$	$2e$	4.399
$Li_4(2,2)$	$2b_1$	4.241
$Li_5(5,0)$	$2b_1$	3.871
$Li_5(4,1)$	$2e$	4.178
$Li_6(6,0)$	$2a_2$	3.822
$Li_6(2,2,2)$	$2b_2$	4.170
$Li_8(6,2)$	$5a_1$	3.778
$Li_9(5,4)$	$5a_1$	3.905

these orbitals are mostly localized about the cluster edge atoms. Therefore, they will be highly affected by edge effects and a large variation of I_{min} with cluster size is a reasonable consequence.

The I_{min} values of Table V are lowered by 0.5–0.8 eV due to relaxation. As an illustration we give the results for Li_9. The frozen orbital I_{min} from Table V, corresponding to ionization out of the $5a_1$ orbital, gives 3.91 eV, whereas the difference of the total energies of the $Li_9(^2A_1)$ ground state and the self-consistent $Li_9^+(^1A_1)$ state (where $5a_1$ is not occupied) gives 3.31 eV. The difference between the two I_{min} values is due to relaxation. One expects that including orbital relaxation $I_{min} \approx 3.5$ eV for all Li_n clusters.

A direct comparison of the I_{min} cluster data with the work function of lithium (100) is problematic. As discussed above, I_{min} is mainly determined by the ionization of orbitals that are localized about edge atoms. In contrast, the concept of work function is based on the idea that electrons of the highest occupied band, states which are not localized on the surface before the ionization, leave the metal. This discrepancy may, but will not necessarily, become smaller as cluster size increases.

The trend of I_{min} towards smaller values with increasing cluster size is consistent with the experimental data. The measured first ionization potential for the atom is 5.39 eV,[56] for Li_2 it is 4.86 eV,[57] and[57] for Li_3 it is 4.35 eV (the average work function of Li metal is 2.48 eV).[58] (However, the experimental data refer to molecules at equilibrium geometry which in the case of Li_2 means an internuclear separation smaller by 20% compared to the value used here.)

A more detailed study of the electronic structure of the different atoms in Li_n is possible if we use Mulliken's population analysis.[59] Table VI shows the charge of the cluster atoms for all Li_n clusters determined by a gross population analysis. For each cluster, symmetry inequivalent atoms are denoted by Li(a), Li(b), Li(c). The data indicate that the atoms remain mostly neutral except in the Li_9 cluster. However, the edge atoms (quantitatively determined by the smallest number of nearest neighbors or the largest mean distance to the other atoms of the cluster) all become slightly negative. The large apparent flow of charge from Li(b) to the four Li(c) atoms in Li_9 is, probably to a large extent, an artifact of the Mulliken gross population analysis. The highest a_1 ($5a_1^1$) MO in Li_9 is a diffuse largely $2s$ orbital which is antibonding between Li(b) and Li(c). The arbitrary partition[59] of the large overlap population for this MO will contribute to the large apparent ionicities in the gross atomic populations.

The flow of charge from the central to the edge atoms can be understood by the Coulomb repulsion of the electrons which makes it energetically more favorable if, starting from a superposition of free-atom charge densities in the cluster, electrons are moved from regions with high initial charge density to those of small density, that is, to those about the edge atoms. Eventually, this charge flow is limited by the nuclear attraction and the exchange interaction about the central atoms. This process is the cluster analog of the formation of a dipole layer at a metal surface.

Table VII gives the distribution of the valence charge in Li_n as well as its decomposition in $2s$ and $2p$ components. (As noted above, the results for the Li_9 cluster are expected to be anomalous because of the large antibonding character of the $5a_1$ MO.) The valence density, which is pure $2s$ in the free atom, acquires $2p$ character in the cluster when Li-Li bonds are formed. The large differences in the $2s$-$2p$ mixing for different atoms in the same cluster indicate a considerable change in the character of the local bonds. In particular, the edge atoms always show less $2p$ admixture

TABLE VI. Atomic charges Q for the Li_n clusters as determined by a gross population analysis. For an identification of the symmetry nonequivalent atoms, the composition formula is given in the last column; see also Fig. 2.

Cluster	Q [Li(a)]	Q [Li(b)]	Q [Li(c)]	Composition
Li	0.0	...	...	$1\times$Li(a)
Li_2	0.0	...	...	$2\times$Li(a)
$Li_4(4,0)$	0.0	...	...	$4\times$Li(a)
$Li_4(2,2)$	0.0	...	...	$4\times$Li(a)
$Li_5(5,0)$	0.02	−0.08	...	$4\times$Li(a) + $1\times$Li(b)
$Li_5(4,1)$	−0.02	0.08	...	$4\times$Li(a) + $1\times$Li(b)
$Li_6(6,0)$	−0.01	0.02	...	$4\times$Li(a) + $2\times$Li(b)
$Li_6(2,2,2)$	−0.01	0.02	...	$4\times$Li(a) + $2\times$Li(b)
$Li_8(6,2)$	−0.07	0.08	0.06	$Li_6(6,0) + 2\times$Li(c)
$Li_9(4,5)$	0.09	0.48	−0.21	$Li_5(4,1) + 4\times$Li(c)

TABLE VII. Distribution of the $2s$- and $2p$-valence charge in Li_n as determined by a gross population analysis. The identification of inequivalent atoms is the same as in Table VI.

Cluster	Q_{val} [Li(a)] $2s$	$2p$	Q_{val} [Li(b)] $2s$	$2p$	Q_{val} [Li(c)] $2s$	$2p$	Composition
Li	1.00	0.0	•••	•••	•••	•••	$1\times$Li(a)
Li_2	0.93	0.07	•••	•••	•••	•••	$2\times$Li(a)
$Li_4(4,0)$	0.83	0.17	•••	•••	•••	•••	$4\times$Li(a)
$Li_4(2,2)$	0.75	0.25	•••	•••	•••	•••	$4\times$Li(a)
$Li_5(5,0)$	0.92	0.06	0.74	0.34	•••	•••	$4\times$Li(a) + $1\times$Li(b)
$Li_5(4,1)$	0.83	0.19	0.36	0.56	•••	•••	$4\times$Li(a) + $1\times$Li(b)
$Li_6(6,0)$	0.87	0.13	0.48	0.52	•••	•••	$4\times$Li(a) + $2\times$Li(b)
$Li_6(2,2,2)$	0.77	0.24	0.66	0.32	•••	•••	$4\times$Li(a) + $2\times$Li(b)
$Li_8(6,2)$	0.92	0.15	0.45	0.47	0.44	0.50	$Li_6(6,0)$ + $2\times$Li(c)
$Li_9(4,5)$	0.47	0.44	0.02	0.54	1.08	0.12	$Li_5(4,1)$ + $4\times$Li(c)

than the more central cluster atoms. This can be explained by the fact that the edge atoms see fewer nearest neighbors than central atoms. Thus they form fewer of the directed bonds which require $2p$ admixtures.

Following the simple approach of Jones *et al.*[60] the $2s$-$2p$ admixture of the Li atom in the metal is characterized by $2s^{0.62}2p^{0.38}$. A strict quantitative comparison of this valence structure with cluster values given in Table VII is not too meaningful because Jones's model for the metal situation as well as the cluster data from a population analysis are rather crude approximations. However, the data indicate considerable discrepancies between the cluster valence structure and the bulk situation.

Fripiat *et al.*[38] have computed wave functions for several Li_n clusters using the MS$X\alpha$ method. However, a comparison with the present work is difficult since their clusters were not chosen to model a (100) surface and, in general, have different geometrical structures than ours. In addition, they varied the Li-Li distance in order to minimize the total statistical energy of their clusters, while we have kept our distances fixed at appropriate bulk values.

In conclusion, the present results show that our Li_n clusters are too small to represent a bulklike electronic situation. The influence of edge effects is always quite large as can be seen from the local electronic structure, the binding energies of the cluster atoms, and the first ionization potentials. The interaction of oxygen with Li_n should converge more rapidly as the cluster size is increased because the oxygen-lithium surface interaction is considered to be a strongly localized phenomenon. In the cluster model, the adsorption properties are determined by differences in the properties of the two systems Li_nO and $(Li_n + O_{atom})$. In this case, we expect the difference between Li_n and the metal surface to cancel to a first approximation.

B. Li_nO clusters (oxygen on-top position)

We have modeled the interaction of an oxygen atom in the on-top position with the clusters LiO, $Li_5(5,0)$, and $Li_9O(5,4)$ (cf. Sec. IIA and Fig. 2). The results for the respective cluster ground-state configuration, the oxygen equilibrium distance, and binding energy are given in Table VIII for LiO and Li_9O. In both clusters the oxygen equilibrium distance d_{min} with respect to the nearest lithium is roughly the same ($d_{min} \approx 3.2a_0$). For $Li_5O(5,0)$ no energetically stable state was found between $d = 2a_0$ and $d = 4a_0$ [for $d = 3.2a_0$, the lowest Li_5O state ^2E lies $\approx$2 eV above the dissociation limit $Li_5(^4B_2) + O(^3P)$]. This result should be due to the poor Hartree-Fock description of the Li-Li interaction at large distances and the particular geometry of the Li_5 substrate. This problem leads in the pure Li_5 substrate cluster to a quite weakly bound state of high spin multiplicity. For these reasons, we do not include the $Li_5O(5,0)$ results in our discussion.

The oxygen binding energy D does not differ substantially between LiO ($D = 1.708$ eV) and Li_9O ($D = 1.231$ eV). Together with the almost identical equilibrium distance d_{min}, this suggests a similar oxygen-lithium binding situation in both clusters which is confirmed by a more detailed study of the electronic structure.

Table IX shows the charge situation of the different cluster atoms derived from the gross population analysis. In both clusters there is a charge transfer of ~0.8 electrons towards the oxygen which indicates a mostly ionic adsorbate-substrate bond. Thus, the clusters can be roughly characterized as Li^+O^- and $(Li_9)^+O^-$. Further, the data in Table IX suggest that in $Li_9O(5,4)$ the charge in-

TABLE VIII. Properties of the ground states of the Li_nO clusters for O at the equilibrium distance d_{min} from the surface. The ground-state configuration, the equilibrium distance, and the oxygen binding energy D are given. The binding energy for Li_nO is defined as the Hartree-Fock energy of Li_nO for O at d_{min} less the energies of Li_n and the $O(^3P)$ atom. The configuration is specified by giving the last orbital in each irreducible representation. The clusters are grouped according to the adsorption site used.

Oxygen site	Cluster	Point-group symmetry	Ground state	Configuration	d_{min} (bohrs)	D (eV)
On top	LiO	$C_{\infty v}$	$^2\Pi$	$4\sigma^2 1\pi^3$	3.206	1.708
	$Li_9O(5,4)$	C_{4v}	$^2A_1$	$7a_1^1 2b_1^2 1b_2^2 4e^4$	3.247	1.231
Central	$Li_4O(4,0)$	$C_{4v}(D_{4h})$ [a]	^3E	$5a_1^1 3e^1 1b_2^2$	0.0	1.946
	$Li_5O(4,1)$	C_{4v}	^2E	$6a_1^2 3e^1 1b_2^2$	−0.042	3.163
	$Li_9O(4,5)$	C_{4v}	$^2B_1$	$7a_1^2 2b_1^1 1b_2^2 4e^4$	−0.016	3.000
Bridge	$Li_2O(2,0)$	$C_{2v}(D_{\infty h})$ [a]	$^1A_1$	$4a_1^2 2b_1^2 1b_2^2$	0.0	3.479
	$Li_6O(6,0)$	$C_{2v}(D_{2h})$ [a]	$^1A_1$	$6a_1^2 3b_1^2 3b_2^2 1a_2^2$	0.0	2.220
	$Li_4O(2,2)$	$C_{2v}(S_4)$ [a]	$^1A_1$	$6a_1^2 2b_1^2 2b_2^2$	−1.654	5.134
	$Li_8O(6,2)$	C_{2v}	$^3B_2$	$7a_1^2 4b_1^1 4b_2^2 2a_2^1$	−1.845	5.759
	$Li_6O(2,2,2)$	C_{2v}	$^3A_2$	$7a_1^2 4b_1^1 3b_2^1$	−1.068	4.960

[a] The cluster for oxygen at d_{min} has the higher symmetry shown in parenthesis. The oxygen geometry optimization was carried out for points with lower total cluster symmetry.

crease on the oxygen is combined with a charge decrease of the same amount on the lithium directly below the oxygen [Li(a)], whereas the other lithiums remain more or less neutral. This corresponds to the situation in a diatomic LiO which is only slightly perturbed by the surrounding eight lithium atoms. In order to get information about the charge rearrangement in the clusters when the oxygen atom is adsorbed, we may compare the situations in Li_nO and the respective Li_n cluster. The results given in Table X show that in $Li_9O(5,4)$ the five lithiums of the first layer [Li(a), Li(b)] all lose 0.3–0.4 electrons to increase the charge on both the oxygen and to some extent on the lithiums

TABLE IX. Gross atomic charges Q as determined from a Mulliken population analysis for the Li_nO clusters for O at d_{min}. The symmetry inequivalent Li atoms are identified by a composition formula. (The definitions for $Li_9O(5,4)$, $Li_4O(2.2)$, and $Li_6O(2.2.2)$ differ from those used in Tables VI and VII for the bare Li_n clusters.)

Site	Cluster	Q (O)	Q [Li(a)]	Q [Li(b)]	Q [Li(c)]	Composition
On top	LiO	−0.81	+0.81 [a]	···	···	O + Li(a)
	$Li_9O(5,4)$	−0.88	+0.92 [a]	+0.09 [a]	−0.10 [b]	O + Li(a) + 4×Li(b) + 4×Li(c)
Central	$Li_4O(4,0)$	−1.54	+0.39 [a]	···	···	O + 4×Li(a)
	$Li_5O(4,1)$	−1.52	+0.24 [a]	+0.59 [b]	···	O + 4×Li(a) + Li(b)
	$Li_9O(4,5)$	−1.56	+0.42 [a]	+0.76 [b]	−0.22 [b]	$Li_5O(4,1)$ + 4×Li(c)
Bridge	$Li_2O(2,0)$	−1.52	+0.76 [a]	···	···	O + 2×Li(a)
	$Li_6O(6,0)$	−1.50	+0.68 [a]	+0.03 [a]	···	O + 2×Li(a) + 4×Li(b)
	$Li_4O(2,2)$	−1.71	+0.43 [a]	+0.43 [b]	···	O + 2×Li(a) + 2×Li(b)
	$Li_8O(6,2)$	−1.72	+0.53 [a]	−0.18 [a]	+0.72 [b]	$Li_6O(6,0)$ + 2×Li(c)
	$Li_6O(2,2,2)$	−1.68	+0.60 [a]	+0.45 [b]	−0.21 [c]	O + 2×Li(a) + 2×Li(b) + 2×Li(c)

[a] Atom in the first layer of the cluster.
[b] Atom in the second layer of the cluster.
[c] Atom in the third layer of the cluster.

TABLE X. Changes in gross atomic charge ΔQ between Li_nO and Li_n plus O. We define $\Delta Q = Q(Li_nO) - Q(Li_n + O)$. The inequivalent Li atoms are identified as in Table IX.

Site	Cluster	ΔQ(O)	ΔQ[Li(a)]	ΔQ[Li(b)]	ΔQ[Li(c)]
On top	LiO	−0.81	+0.81 [a]	•••	•••
	$Li_9O(5,4)$	−0.88	+0.44 [a]	+0.30 [a]	−0.19 [b]
Central	$Li_4O(4,0)$	−1.54	+0.39 [a]	•••	•••
	$Li_5O(4,1)$	−1.52	+0.26 [a]	+0.51 [b]	•••
	$Li_9O(4,5)$	−1.56	+0.33 [a]	+0.28 [b]	−0.01 [b]
Bridge	$Li_2O(2,0)$	−1.52	+0.76 [a]	•••	•••
	$Li_6O(6,0)$	−1.50	+0.66 [a]	+0.04 [a]	•••
	$Li_4O(2,2)$	−1.71	+0.43 [a]	+0.43 [b]	•••
	$Li_8O(6,2)$	−1.72	+0.45 [a]	−0.11 [a]	+0.66 [b]
	$Li_6O(2,2,2)$	−1.68	+0.61 [a]	+0.43 [b]	−0.20 [c]

[a] First layer atom. [b] Second layer atom. [c] Third layer atom.

of the second layer [Li(c)]. This rearrangement accounts for the difference in the binding energy between LiO and Li_9O. The charge increase on the Li(c) seems to be a consequence of the edge effect.

The valence charge on the cluster atoms and its decomposition into 2s and 2p contributions is given in Table XI. The data show that the charge increase on the oxygen in LiO and Li_9O is caused by the occupation of cluster orbitals with mostly oxygen 2p character. This is consistent with the fact that the energetically lowest available orbitals in the oxygen atom are 2p orbitals.

More quantitative information about the charge distribution in the clusters requires a detailed knowledge of the electronic structure which goes far beyond a population analysis. In general, the population analysis data given in Tables IX–XI are to be taken only qualitatively. First, the decomposition of the cluster electronic charge into atomic contributions is problematic because in the strict sense there are no separate atoms in a cluster. Second, in the gross population analysis the partitioning of electronic charge is quantitatively meaningful only if the basis functions of different

TABLE XI. Decomposition of the gross atomic populations of Li_nO into 2s and 2p character. Both Li and O are assumed to have $1s^2$ cores. The identification of the inequivalent Li atoms is as given in Table IX.

		Q(O)		Q[Li(a)]		Q[Li(b)]		Q[Li(c)]	
Site	Cluster	2s	2p	2s	2p	2s	2p	2s	2p
On top	LiO	1.98	4.83	0.02	0.17	•••	•••	•••	•••
	$Li_9O(5,4)$	1.99	4.89	0.12	0.07	0.80	0.09	0.67	0.42
Central	$Li_4O(4,0)$	1.95	5.59	0.42	0.19	•••	•••	•••	•••
	$Li_5O(4,1)$	1.95	5.57	0.62	0.14	0.13	0.28	•••	•••
	$Li_9O(4,5)$	1.95	5.61	0.28	0.30	0.00	0.24	1.10	0.12
Bridge	$Li_2O(2,0)$	1.93	5.59	0.02	0.22	•••	•••	•••	•••
	$Li_6O(6,0)$	1.93	5.57	0.07	0.25	0.93	0.04	•••	•••
	$Li_4O(2,2)$	1.94	5.77	0.53	0.04	0.53	0.04	•••	•••
	$Li_8O(6,2)$	1.94	5.78	0.08	0.39	1.05	0.13	0.07	0.21
	$Li_6O(2,2,2)$	1.94	5.74	0.18	0.22	0.37	0.18	0.94	0.27

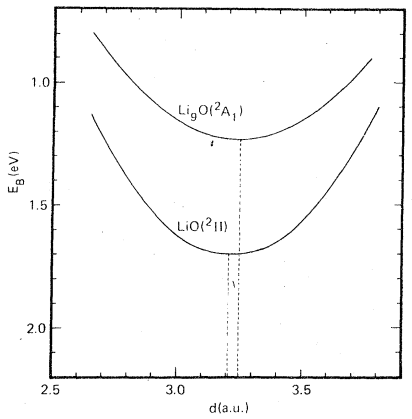

FIG. 4. Oxygen binding energy as a function of distance d for the on-top site.

atomic centers do not overlap, which usually holds only for the most contracted basis functions.

Figure 4 shows the binding curve as a function of the oxygen distance d near equilibrium distance for both LiO and $Li_9O(5,4)$. From these curves we determine the parameters for oxygen vibrations perpendicular to the surface. The results are given in Table XII. For a comparison, we suppose that the lithium part is rigidly connected to the rest of the substrate with infinite mass. The vibrational energy $\hbar\omega$ is given, in the harmonic approximation, by

$$\hbar\omega = \hbar(\kappa/m_0)^{1/2},$$

where κ is the curvature of the respective binding curve at equilibrium distance and m_0 the mass of the oxygen. The value of $\hbar\omega$ decreases, analogously to the binding energy, from LiO to $Li_9O(5,4)$ by only 20%. This gives further indication of a similar binding situation in the two clusters.

If we take into account the finite lithium mass in $^7Li^{16}O$ we find $\hbar\omega = 838$ cm^{-1} (the Hartree-Fock limit is $\hbar\omega = 840.4$ cm^{-1}).[52] Our results are in good agreement with extended CI calculations[52] which give $\hbar\omega = 825.2$ cm^{-1}, while spectroscopic data of $^7Li^{16}O$ embedded in a krypton matrix yield $\hbar\omega = 745$ cm^{-1}.[61] The difference between calculation and experiment is sufficiently explained by the interaction of the molecule with the matrix.

In conclusion, the two Li_nO clusters for the oxygen on top position are quite similar in their oxygen-lithium interaction. This is obvious from the results for the oxygen equilibrium distance ($d_{min} \approx 3.2a_0$), the binding energy ($D \approx 1.25$–1.7 eV), and the vibrational data ($\hbar\omega \approx 390$–460 cm^{-1}). Further, the population analysis indicates that the oxygen becomes ionic (O^-) in the clusters.

C. Li_nO clusters (oxygen central position)

The interaction of oxygen in the central position is modeled with the clusters $Li_4O(4,0)$, $Li_5O(4,1)$, and $Li_9O(4,5)$ (cf. Sec. IIA and Fig. 2). The results for the ground states and the oxygen binding are given in Table VIII. In the three clusters the oxygen always stabilizes in the plane through the lithium centers of the first layer ($d_{min} \approx 0$). However, the oxygen binding energy differs significantly between Li_4O ($D \approx 1.9$ eV), Li_5O, and Li_9O ($D \approx 3$ eV). This difference can be explained by the geometry of the clusters. Both Li_5O and Li_9O contain lithium atoms of the second layer, whereas

TABLE XII. Parameters for oxygen vibration perpendicular to the surface and computed in a harmonic approximation. Here κ is the curvature of the Li_nO binding curve at equilibrium distance. The vibrational energies $\hbar\omega$ are determined for a rigid lithium cluster Li_n assumed to have infinite mass. and ^{16}O.

Site	Cluster	κ (hartree/a_0^2)	$\hbar\omega$ (cm^{-1}, meV)
On top	LiO	0.12870	461, 57.2
	$Li_9O(5,4)$	0.08962	385, 47.7
Central	$Li_4O(4,0)$	0.03172	229, 28.4
	$Li_5O(4,1)$	0.11481	435, 54.0
	$Li_9O(4,5)$	0.10308	413, 51.2
Bridge	$Li_2O(2,0)$	0.02930	220, 27.3
	$Li_6O(6,0)$	0.02378	198, 24.6
	$Li_4O(2,2)$	0.03570	243, 30.1
	$Li_8O(6,2)$	0.04211	263, 32.7
	$Li_6O(2,2,2)$	0.02821	216, 26.8

$Li_4O(4,0)$ does not. In particular, the central lithium of the second layer which is nearest to the oxygen in its stable position is not present in Li_4O. This must necessarily weaken the oxygen-lithium binding.

The electronic structure of the three clusters as derived from the population analysis is given in Tables IX–XI. Table IX shows that in the three clusters there is a charge transfer of 1.5 electrons towards the oxygen. The charge of the clusters is roughly characterized by $(Li_4)^{2+}O^{2-}$, $(Li_5)^{2+}O^{2-}$, and $(Li_9)^{2+}O^{2-}$. This suggests an adsorbate-substrate bond with a stronger ionic contribution than for the Li_nO clusters of the oxygen on-top position. As expected, the charge increase on the oxygen is caused by the occupation of cluster orbitals with mostly oxygen $2p$ character (see Table XI).

Table X shows the charge rearrangement in the clusters due to the oxygen-lithium interaction. In $Li_5O(4,1)$ the central lithium of the second layer [Li(b)] loses more charge than each of the four lithiums of the first layer [Li(a)]. For $Li_9O(4,5)$, which is increased by four atoms of the second layer [Li(c)] with respect to $Li_5O(4,1)$, the four atoms Li(a), and the atom Li(b) seem to lose roughly the same charge, whereas the four atoms Li(c) keep their Li_9 charge state in Li_9O. Although these results are affected by the uncertainty of the population analysis discussed above, they clearly show the importance of the central lithium atom of the second layer Li(b) for the adsorbate-substrate interaction.

Figure 5 shows the oxygen binding energy D as a function of the distance d near equilibrium distance for the three clusters. The parameters for oxygen vibrations perpendicular to the surface

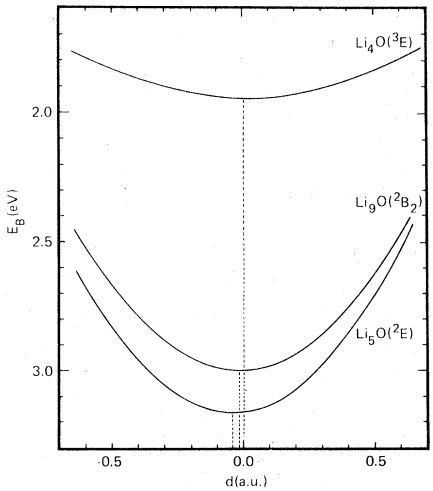

FIG. 5. Oxygen binding energy as a function of distance d for the central site.

calculated from $D(d)$ are given in Table XII where, as before, an infinite mass for the lithium cluster part was assumed. The energies $\hbar\omega$ in $Li_5O(4,1)$ and $Li_9O(4,5)$ are roughly identical, whereas $\hbar\omega$ is smaller by almost 50% in $Li_4O(4,0)$. The difference is explained by the lack of the central Li(b) atom in Li_4O which should affect the oxygen vibration strongly because the Li(b) lies on the axis of vibration. In Li_9O, the four lithiums of the second layer Li(r) (by which Li_9O differs from Li_5O) do not influence the oxygen vibration; this is as one would expect from geometry arguments.

In conclusion, we find for the three clusters of the oxygen central position that the oxygen center stabilizes in the plane through the lithium centers of the first layer ($d_{min} \approx 0$) as roughly O^{2-}. The binding energies and the vibrational results are quite similar for $Li_5O(4,1)$ and $Li_9O(4,5)$ ($D \approx 3$ eV, $\hbar\omega \approx 420$ cm^{-1}), whereas they differ substantially for $Li_4O(4,0)$ ($D \approx 1.9$ eV, $\hbar\omega \approx 230$ cm^{-1}). This is explained by the lack of the central lithium of the second layer in Li_4O.

D. Li_nO clusters (oxygen bridge position)

Five clusters, $Li_2O(2,0)$, $Li_4O(2,2)$, $Li_6O(2,2,2)$, $Li_6O(6,0)$, and $Li_8O(6,2)$, are used to model the interaction of the oxygen in the bridge position (cf. Sec. IIA and Fig. 2). Table VIII gives the results for the cluster ground states and the oxygen binding. For both $Li_2O(2,0)$ and $Li_6O(6,0)$ the oxygen equilibrium distance d_{min} becomes zero, that is, $Li_2O(2,0)$ is linear at its equilibrium[62] and $Li_6O(6,0)$ is planar. In the other three clusters, which include lithium atoms of the second layer, the oxygen stabilizes between the first and the second lithium layer ($d_{min} < 0$). Interestingly, in $Li_6O(2,2,2)$ with the oxygen in the symmetry center of the lithium octahedron (corresponding to an oxygen in the second lithium layer), we could not find a cluster state that was energetically lower than the one given in Table VIII where the oxygen is "asymmetric" and well above the second Li layer. However, this does not exclude the possibility that in larger clusters the oxygen stabilizes at or below the second layer of lithium atoms.

The results of the oxygen binding energy D suggest the same grouping of the clusters as is found for the equilibrium position. Both $Li_2O(2,0)$ and $Li_6O(6,0)$ give considerably lower binding energies ($D = 3.5$ eV and $D = 2.2$ eV) compared to the rest of the clusters. $Li_6O(2,2,2)$ differs from $Li_4O(2,2)$ only slightly in the binding energy ($D \approx 5.0$ eV compared to 5.1 eV), and $Li_8O(6,2)$ has the largest value ($D = 5.8$ eV).

The considerable differences between the two

groups of clusters concerning their oxygen binding energies as well as their equilibrium positions show the importance of the second-layer lithium atoms for the adsorbate-substrate interaction in the bridge position as has been shown above for the central position.

The gross population data of Table IX show that in all five clusters the oxygen contains an excess charge of 1.5–1.7 electrons caused by the occupation of oxygen $2p$-like cluster orbitals (cf. Table XI). Thus, the charge situation in these clusters is roughly characterized by $(Li_n)^{2+}O^{2-}$ which indicates a highly ionic adsorbate-substrate bond comparable to the bond in the clusters of the central position.

In $Li_4O(2,2)$ the excess charge on the oxygen which stabilizes in the symmetry center of the lithium tetrahedron comes from all four lithiums equally. Obviously, this leads to a stronger oxygen-lithium binding than in $Li_2O(2,0)$ or $Li_6O(6,0)$ where only two neighboring lithiums contribute to the charge transfer towards the oxygen (cf. Tables IX and X). In $Li_6O(2,2,2)$ the stable oxygen position is shifted towards the two lithiums of the first layer [Li(a)] compared to the situation in $Li_4O(2,2)$. This shift affects the oxygen charge only slightly, whereas the [Li(a)] atoms become more positive compared to Li_4O, the lithiums of the second layer [Li(b)] keep their Li_4O charge, and the lithiums of the third layer [Li(c)] become slightly negative. The latter result is interpreted as an edge effect. In $Li_8O(6,2)$ the oxygen ionicity is roughly identical to that in $Li_4O(2,2)$. The central lithiums of the first and second layer [Li(b) and Li(c)] become more positive than in Li_4O, whereas the four outer lithiums of the first layer [Li(a)] are slightly negative which again seems to be an edge effect.

Figure 6 shows the oxygen binding curves $D(d)$ for the three clusters that include lithium atoms in the second (and third) layer. The oxygen vibration parameters computed from these curves are given in Table XII. Here the grouping of the clusters, which is obvious in the binding-energy and equilibrium position results, is much less pronounced. The energies $\hbar\omega$ for $Li_4O(2,2)$ and $Li_8O(6,2)$ are slightly increased compared to those for $Li_2O(2,0)$ and $Li_6(6,0)$, but the $\hbar\omega$ value for $Li_6(2,2,2)$ (which compares to Li_4O and Li_8O with respect to D and d_{min}) is almost identical to the value for $Li_2O(2,0)$. However, the values for all clusters are reasonably close to each other.

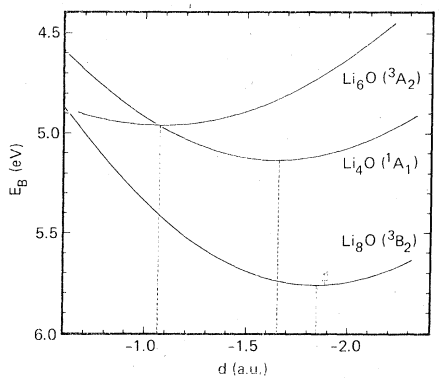

FIG. 6. Oxygen binding energy as a function of distance d for the bridge site.

In conclusion, the oxygen binding data support a division of the five clusters for the bridge position into two groups. In the first group, consisting of $Li_2O(2,0)$ and $Li_6O(6,0)$, only lithium atoms of the first layer are taken into account. As a consequence these clusters are linear (planar) in the oxygen equilibrium with oxygen binding energies $D = 3.5$ eV (2.2 eV). The clusters of the second group, $Li_4O(2,2)$, $Li_6O(2,2,2)$, and $Li_8O(6,2)$, all include lithium atoms of the second layer. Here the oxygen stabilizes as O^{2-} between the first and the second lithium layer with a binding energy (5.1, 5.0, and 5.8 eV) which is considerably higher compared to the values of the first group. This indicates the importance of including lithium atoms of the second layer for describing the adsorbate-substrate interaction in the bridge position. The results for oxygen vibrations perpendicular to the surface are roughly the same for all five clusters.

IV. CONCLUSIONS FOR ADSORPTION OF O ON Li(100)

The oxygen-lithium interaction differs significantly among the three high-symmetry positions of the surface as has been discussed in Secs. III B–III D. In the following we summarize the most important cluster results and discuss possible consequences for the situation on the Li(100) surface.

The oxygen on-top position is energetically least favorable. Here the oxygen stabilizes at $d_{min} = 3.2a_0$ (corresponding to half a lattice constant of Li metal) above the first lithium layer with binding energy $D = 1.25$ eV for Li_9O and $D = 1.7$ eV for LiO. The small difference in d_{min} between LiO and $Li_9O(5,4)$ strongly suggests that similar results will be obtained for much larger clusters. The variation of the binding energy with cluster size is somewhat larger. However, clusters larger than Li_9O are not likely to have significantly different oxygen binding energies since the added Li atoms will be at large distances from the oxygen. Thus, it is reasonable to accept a value of $D \approx 1.25$ eV for Hartree-Fock calculations for the on-top site.

In the clusters which model oxygen adsorbed in

the central and bridge sites, the lithium atoms of the second layer are quite important for a proper description of the oxygen-lithium interaction. Thus, only those clusters are included in the discussion below.

In the central position clusters, the oxygen becomes stable in the first lithium layer ($d_{min} \approx 0$) with a binding energy $D \approx 3$ eV which is considerably higher than for the on-top position. Both d_{min} and D differ only slightly between $Li_5O(4,1)$ and $Li_9O(4,5)$, which strongly suggests similar results if the cluster size is further increased.

The oxygen bridge position is energetically most favorable. Here the adsorbate stabilizes between the first and the second lithium layer with a binding energy $D \approx 5$ to 6 eV. For this symmetry position one expects the largest variations in the oxygen binding if the cluster size is further increased. In particular it could be possible that the oxygen penetrates even further into the substrate in larger clusters. However, the result that the oxygen penetrates into the substrate with a binding energy well above the central and on-top position values should also be valid for larger clusters.

The present binding energies D differ from the Hartree-Fock limit by approximately 0.2 eV due to the restricted basis set (cf. Sec. IIC). Additional contributions to D are caused by correlation effects. Extended CI calculations on LiO show[52] an increase in the binding energy of 1.5 eV. This correction might be slightly larger in the Li_nO clusters of the central and bridge position because of the higher oxygen ionicity. Thus, we estimate that our results for D should be too small by roughly 1–2 eV due to the neglect of correlation effects. However, the correlation corrections should not be so different for the different sites that the order

$$D_{\text{on top}} < D_{\text{central}} < D_{\text{bridge}}$$

of the oxygen binding energies would be changed.

The orbital structures and population analyses show that in all clusters the oxygen is ionic: O^- in the on top position and O^{2-} in the central and bridge position. This indicates a highly ionic oxygen-lithium bond where the binding energy increases with ionicity. The charge situation of the oxygen in the bridge position is comparable to the situation in the Li_2O ionic crystal. There the oxygen has eight nearest-neighbor lithiums in cubic arrangement[40] and is roughly 0^{2-}. This is also found in Hartree-Fock calculations of a Li_8O^{6+} cluster in a Madelung environment.[65]

Quinn and Richardson[39] have reported results for Li_nO clusters ($n \leq 5$) using the MS$X\alpha$ method. Their primary interest was to investigate the changes in core and valence level ionization potentials resulting from adding fractional numbers of electrons to the clusters. They considered two sites, central and on top, on the (100) surface of lithium. The central site was modeled with a $Li_4O(4,0)$ cluster and the on-top site with $Li_5O(5,0)$ and LiO clusters. They did not optimize the distance of the O atom from the cluster, but used distances of 6.61 and 4.72 bohrs for the on top site and 4.72 bohrs for the central site. Our results raise serious doubts about the ability of their clusters to describe the interaction of the oxygen adatom with the substrate. In particular, the oxygen to lithium distances which they chose are, for both sites considered, much too large. Further, for the central site, we have shown that it is important to include lithium atoms in the second layer, which Quinn and Richardson have not done. Finally, the $Li_5O(5,0)$ cluster, which, in our calculations, did not give a bound state for oxygen, is probably a poor choice for studying the on-top site.

The results for oxygen vibrations perpendicular to the surface are different for two different groups of clusters. The first group comprises all clusters where the oxygen vibrates against a lithium center, that is, those for the on-top and central position. Here the vibrational energy $\hbar\omega (\cong 53$ meV) is larger by a factor of 1.75 compared to the second group of clusters, those for the bridge position where no lithium center lies on the axis of vibration ($\hbar\omega \cong 30$ meV). This result cannot be explained by a model which has been used by Froitzheim *et al.* to interpret vibrational excitations of adsorbed oxygen[66] and hydrogen[67] on a tungsten surface. They assumed that the adsorbate vibration is mainly determined by a superposition of springs connecting the adsorbate with nearest substrate surface atoms where the sum of the effective force constants is independent of the adsorbate site. Although cluster calculations have shown that this sum rule holds for H on Be(0001),[29,68] it is clear that it does not apply to O on Li(100). This may be related to the fact that the binding energies at the different sites for O on Li(100) are very different.

Our cluster results indicate that the adsorption of oxygen on a Li(100) can be described as follows. The oxygen binding to the surface is weaker for the on-top than for the central position and is most stable in the bridge position where oxygen penetrates into the crystal. In this site, it is highly ionic (O^{2-}) which leads to an ionic bonding comparable to the situation in the ionic crystal Li_2O. This interaction model is consistent with the experimental situation. As mentioned above, lithium metal reacts spontaneously with oxygen gas to form lithium oxide (Li_2O). This reaction requires a preferable penetration of oxygen atoms into the

metal where the energy gain per oxygen atom should be greater than 50% of the dissociation energy of the O_2 molecule (2.56 eV).[69] Both conditions are found for the bridge site clusters. However, for a detailed description of the complete oxidation process changes in local surface structure have to be considered. Further, the adsorbate-adsorbate interaction can become important in the real case. Both effects seem to be very difficult to describe in cluster models as they would require multidimensional geometry optimizations in considerably larger clusters. Studies of this kind might become possible with semiempirical methods (complete neglect of differential overlap, extended Hückel theory), where the adjustable parameters could be determined from the present *ab initio* calculations. Experimental studies of the oxidation of well-defined lithium surfaces which, to our knowledge, have not been carried out yet could provide further useful information towards an understanding of the oxidation process.

---

*Permanent address: Institute für Theoretische Physik B, TU Clausthal, 3392 Clausthal-Zfd., West Germany.

[1]J. R. Smith, S. C. Ying, and W. Kohn, Phys. Rev. Lett. 30, 610 (1973); S. C. Ying, J. R. Smith, and W. Kohn, Phys. Rev. B 11, 1483 (1975).

[2]N. D. Lang and A. R. Williams, Phys. Rev. Lett. 34, 531 (1975).

[3]O. Gunnarsson and H. Hjelmberg, Phys. Scr. 11, 97 (1975).

[4]J. A. Appelbaum and D. R. Hamann, Phys. Rev. Lett. 34, 806 (1975).

[5]R. V. Kasowski, Phys. Rev. Lett. 37, 219 (1976).

[6]K. M. Ho, M. L. Cohen, and M. Schlüter, Phys. Rev. B 15, 3888 (1977).

[7]K. C. Pandey, Phys. Rev. B 14, 1557 (1976).

[8]I. P. Batra and S. Ciraci, *Proceedings of the Seventh International Vacuum Congress and the Third International Conference on Solid Surfaces, Vienna, 1977* edited by R. Dobrozemsky, F. Rüdenauer, F. P. Viehböck, and A. Breth (Dobrozemsky, Vienna, 1977), p. 1141.

[9]P. W. Anderson, Phys. Rev. 124, 41 (1961).

[10]J. Hubbard, Proc. R. Soc. (London) 277, 237 (1964).

[11]T. B. Grimley, Prog. Surf. Membr. Sci. 9, 71 (1975).

[12]J. R. Schrieffer and R. Gomer, Surf. Sci. 25, 315 (1971).

[13](a) T. B. Grimley, in *Proceedings of the International School of Physics, Enrico Fermi, Course LVIII*, edited by F. O. Goodman, (Editrice Compositori, Bologna, 1974), p.298; (b) J. R. Schrieffer, *ibid.*, p. 250; (c) T. B. Grimley, *NATO Advanced Study Institutes Series, Series B: Physics* (Plenum, New York, 1976), Vol. 16, p. 113.

[14]T. B. Grimley, in *Molecular Processes on Solid Surfaces* (McGraw-Hill, New York, 1969).

[15]T. B. Grimley and C. Pisani, J. Phys. C 7, 2831 (1974).

[16]A. J. Bennett, B. McCarroll, and R. P. Messmer, Surf. Sci. 24, 191 (1971); Phys. Rev. B 3, 1397 (1971).

[17]D. J. M. Fassaert, H. Verbeek, and A. van der Avoird, Surf. Sci. 29, 501 (1972).

[18]L. W. Anders, R. S. Hansen, and L. S. Bartell, J. Chem. Phys. 59, 5277 (1973).

[19]L. W. Anders, R. S. Hansen, and L. S. Bartell, J. Chem. Phys. 62, 1641 (1975).

[20]J. C. Robertson and C. W. Wilmsen, J. Vac. Sci. Technol. 9, 901 (1972).

[21]G. Blyholder, J. Chem. Phys. 62, 3193 (1975).

[22]T. B. Grimley and E. E. Mola, J. Phys. C 9, 3437 (1976).

[23]W. Brunn, L. Fritsche, and K. Hermann, Int. J. Quantum Chem. Symp. 8, 483 (1974).

[24]For a review see, N. Rösch, in Ref. 13c, 1976.

[25]J. T. Waber, H. Adachi, F. W. Averill, and D. E. Ellis, Jpn. J. Appl. Phys. Suppl. 2, 695 (1974).

[26]D. E. Ellis, H. Adachi, and F. W. Averill, Surf. Sci. 58, 497 (1976).

[27]C. W. Bauschlicher, D. H. Liskow, C. F. Bender, and H. F. Schaefer III, J. Chem. Phys. 62, 4815 (1975).

[28]C. W. Bauschlicher, C. F. Bender, H. F. Schaefer III, and P. S. Bagus, Chem. Phys. 15, 227 (1976).

[29]C. W. Bauschlicher, P. S. Bagus, and H. F. Schaefer III, IBM J. Res. Dev. (to be published).

[30]L. S. Cederbaum, W. Domcke, W. von Niessen, and W. Brenig, Z. Phys. B 21, 381 (1975).

[31]P. S. Bagus and K. Hermann, Solid State Commun. 20, 5 (1976).

[32]K. Hermann and P. S. Bagus, Phys. Rev. B 16, 4195 (1977).

[33]C. F. Melius, J. M. Moskowitz, A. P. Mortola, M. B. Baillie, and M. A. Ratner, Surf. Sci. 59, 279 (1976).

[34]K. Hermann, in Ref. 8, p. 943.

[35]R. P. Messmer, S. K. Knudson, K. H. Johnson, J. B. Diamond, and C. Y. Yang, Phys. Rev. B 13, 1396 (1976).

[36]C. E. Sessions and J. H. DeVan, Nucl. Appl. Technol. 9, 250 (1970).

[37]E. F. Cairns, F. A. Cafasso, and V. A. Maroni, in *The Chemistry of Fusion Technology*, edited by D. M. Gruen (Plenum, New York, 1972).

[38]J. G. Fripiat, K. T. Chow, M. Boudart, J. B. Diamond, and K. H. Johnson, J. Mol. Catal. 1, 59 (1976).

[39]C. M. Quinn and N. V. Richardson, Faraday Discuss. Chem. Soc. 60, 201 (1976).

[40]R. W. G. Wyckoff, *Crystal Structures*, 2nd ed. (Interscience, New York, 1964), Vol. II.

[41]C. B. Duke, N. O. Lipari, and G. E. Laramore, Nuovo Cimento B 23, 241 (1974).

[42]C. C. J. Roothaan, Rev. Mod. Phys. 23, 69 (1951).

[43]C. C. J. Roothaan, Rev. Mod. Phys. 32, 179 (1960); C. C. J. Roothaan and P. S. Bagus, Methods Comput. Phys. 2, 47 (1963).

[44]H. F. Schaefer III, *The Electronic Structure of Atoms and Molecules* (Addison-Wesley, Reading, Mass., 1972).

[45]The MOLALCH program package incorporates the MOLECULE integral program and the ALCHEMY SCF program. MOLECULE was written by Dr. J. Almlöf of the University of Uppsala, Sweden. The ALCHEMY SCF program was written by Dr. P. S. Bagus and Dr. B. Liu of the

IBM Research Laboratory, San Jose. The interfacing of these programs was performed by Dr. U. Wahlgren, University of Uppsala and Dr. P. S. Bagus at IBM. The wave-function contour plot part was written by Dr. K. Hermann.

[46]F. B. van Duijneveldt, IBM Research Report No. RJ 945, 1971 (unpublished).

[47]T. H. Dunning, J. Chem. Phys. 53, 2823 (1970).

[48]P. S. Bagus, B. Liu, and H. F. Schäefer III, Phys. Rev. A 2, 555 (1970).

[49]J. E. Williams (unpublished); see, Ref. 51.

[50]P. S. Bagus and U. I. Wahlgren, Mol. Phys. 33, 641 (1977).

[51]P. K. Pearson, W. J. Hunt, C. F. Bender, and H. F. Schäefer III, J. Chem. Phys. 58, 5358 (1973).

[52]M. Yoshimine, J. Chem. Phys. 57, 1108 (1972).

[53]Confer G. Das and A. C. Wahl, J. Chem. Phys. 44, 87 (1966).

[54]W. E. Rudge, IBM Research Report No. RJ 539, 1968 (unpublished).

[55]W. Kolos, F. Nieves, and O. Novaro, Chem. Phys. Lett. 41, 431 (1976).

[56]C. E. Moore, *Atomic Energy Levels*, U. S. Natl. Bur. Stand. Ref. Data Ser. (U.S. GPO, Washington, D.C., 1948), Vol. I.

[57]C. H. Wu, J. Chem. Phys. 65, 3181 (1976).

[58]A. J. Dekker, *Solid State Physics* (Macmillan, London, 1967).

[59]R. S. Mulliken, J. Chem. Phys. 23, 1833 (1955); 23, 1841 (1955); 2338 (1955); and 2343 (1955).

[60]H. Jones, N. F. Mott, and H. W. B. Skinner, Phys. Rev. 45, 379 (1934).

[61]D. White, K. S. Seshadri, D. F. Dever, D. E. Mann, and M. J. Linevski, J. Chem. Phys. 39, 2463 (1963).

[62]A complete geometry optimization of the Li_2O molecule using Hartree-Fock–LCAO techniques (see Ref. 63) gives a linear Li-O-Li structure with Li-O distance $3.12a_0$. This value is smaller by only 6% compared to our value. The experimental distance is $3.00a_0$ (see Ref. 64).

[63]R. J. Buenker and S. D. Peyerimhoff, J. Chem. Phys. 45, 3682 (1966).

[64]S. M. Tolmachev, E. S. Zassonn, and N. G. Rambidi, J. Struct. Chem. (USSR) 10, 449 (1969).

[65]K. Hermann (unpublished).

[66]H. Froitzheim, H. Ibach, and S. Lehwald, Phys. Rev. B 14, 1362 (1976).

[67]H. Froitzheim, H. Ibach, and S. Lehwald, Phys. Rev. Lett. 36, 1549 (1976).

[68]P. S. Bagus and C. W. Bauschlicher, in Ref. 8, p. 989.

[69]A. G. Gaydon, *Dissociation Energies and Spectra of Diatomic Molecules* (Chapman and Hall, London, 1968).